


# Quantum Flow Algorithms for Simulating Many-Body Systems on Quantum Computers

Karol Kowalski\* and Nicholas P. Bauman

*Physical Sciences Division, Pacific Northwest National Laboratory, Richland, Washington 99354, USA*

 (Received 15 May 2023; revised 10 October 2023; accepted 30 October 2023; published 16 November 2023)

We conducted quantum simulations of strongly correlated systems using the quantum flow (QFlow) approach, which enables sampling large subspaces of the Hilbert space through coupled variational problems in reduced dimensionality active spaces. Our QFlow algorithms significantly reduce circuit complexity and pave the way for scalable and constant-circuit-depth quantum computing. Our simulations show that QFlow can optimize the collective number of wave function parameters without increasing the required qubits using active spaces having an order of magnitude fewer number of parameters.

DOI: [10.1103/PhysRevLett.131.200601](https://doi.org/10.1103/PhysRevLett.131.200601)

*Introduction.*—The development of quantum computing has grabbed the attention of the many-body chemistry and physics communities with the promise to provide exponential speed-ups over traditional computing for problems such as solving the electronic Schrödinger equation for ground and excited states or the time-dependent equation for studying dynamics. For the electronic problem, the two salient quantum algorithms for determining energetics with the electronic Hamiltonian are quantum phase estimation (QPE) [1–6] and variational quantum eigensolver (VQE) [7–18]. Both algorithms are seized by complexities that prevent routine calculations of meaningful problems that plague traditional computing. These complexities result from the inherently large dimensionality needed to provide accurate and reliable results. For QPE, this manifests in circuit depths far beyond what is achievable in the noisy intermediate-scale quantum (NISQ) device era of quantum computing. For VQE, a measure of complexity is the number of parameters from a given ansatz currently optimized using traditional computing algorithms. The progress in enabling quantum computing technologies is contingent not only on the advances in the design of quantum materials but also on the ability to adapt to new methodological advances in the theory of correlated many-body systems.

The reduction of dimensionality and compression of quantum Hamiltonians has become a crucial area of focus in the realm of quantum computing. In light of this, it is of utmost importance to develop methodologies that aim to compress the correlation effects in smaller spaces that can be handled by current quantum computing resources [19–21]. As such, the authors have devised a coupled cluster (CC)-based downfolding formalism that enables the incorporation of dynamical correlation effects from large Hilbert spaces into manageable effective Hamiltonians for a smaller subspace of the original problem [22]. This Letter describes and provides numerical evidence for a new dimensionality-reducing technique called the quantum flow (QFlow) approach. The QFlow algorithm integrates

the reduced-dimensionality active space variational problems to approximate the ground-state energy of the Hamiltonian operator within a larger subspace of Hilbert space [23].

Within the framework of QFlow formalism, the highest demand for qubits is linked to the number of qubits necessary for the representation of the quantum problem that corresponds to the largest active space incorporated in the flow. Using modest-size active spaces, we demonstrate that QFlow can efficiently recover the corresponding energetics of the full problem. It is a flexible workflow that we expected to play a pivotal role in performing quantum simulations on quantum computers during the transition from NISQ devices to fully fledged error-corrected quantum computing.

*CC theory and quantum flows.*—The CC theory [24–31] has evolved into a one of the most prominent formalisms to describe correlated systems. In the single-reference variant (SR-CC), the ground-state wave function  $|\Psi\rangle$  is defined by the exponential ansatz

$$|\Psi\rangle = e^T |\Phi\rangle, \quad (1)$$

$$T = \sum_{k=1}^{N_A} \frac{1}{(k!)^2} \sum_{\substack{i_1, \dots, i_k \\ a_1, \dots, a_k}} t_{i_1 \dots i_k}^{a_1 \dots a_k} a_{a_1}^\dagger \dots a_{a_k}^\dagger a_{i_1} \dots a_{i_k}, \quad (2)$$

where  $T$  and  $|\Phi\rangle$  represent the cluster operator and reference function. The  $T$  operator is defined by the maximum excitation level ( $N_A$ ), cluster amplitudes  $t_{i_1 \dots i_k}^{a_1 \dots a_k}$ , and creation/annihilation operators  $a_p^\dagger/a_q$  where  $p, q$  stand for the general spin-orbital indices. The indices  $i_j$  ( $a_j$ ) stand for occupied (unoccupied) spin orbitals in the reference function  $|\Phi\rangle$ . Standard CC equations are given by the equations

$$Qe^{-T}He^T|\Phi\rangle = 0, \quad (3)$$

$$\langle\Phi|e^{-T}He^T|\Phi\rangle = E, \quad (4)$$

where  $Q$  is a projection operator onto excited Slater determinants generated by acting with  $T$  on  $|\Phi\rangle$  (the projection onto the reference function is denoted as  $P$ ). Recently, it has been demonstrated that CC energies can be calculated by diagonalizing effective Hamiltonians in a class of complete active spaces (CASs) that are specific to the approximation of the  $T$  operator [23,32,33]. If, in the particle-hole formalism, CAS is generated by the excitation subalgebra ( $\mathfrak{h}$ ), and the cluster operator  $T$  can be partitioned into internal [ $T_{\text{int}}(\mathfrak{h})$ ; producing excitation within CAS] and external [ $T_{\text{ext}}(\mathfrak{h})$ ; producing excitation outside of CAS] parts and  $e^{T_{\text{int}}(\mathfrak{h})}|\Phi\rangle$  represents an exact-type expansion in the CAS, then the CC energy can be obtained as

$$H^{\text{eff}}(\mathfrak{h})e^{T_{\text{int}}(\mathfrak{h})}|\Phi\rangle = Ee^{T_{\text{int}}(\mathfrak{h})}|\Phi\rangle, \quad (5)$$

$$H^{\text{eff}}(\mathfrak{h}) = [P + Q_{\text{int}}(\mathfrak{h})]e^{-T_{\text{ext}}(\mathfrak{h})}He^{T_{\text{ext}}(\mathfrak{h})}[P + Q_{\text{int}}(\mathfrak{h})], \quad (6)$$

where  $Q_{\text{int}}(\mathfrak{h})$  is a projection onto excited (with respect to  $|\Phi\rangle$ ) configurations in the CAS. The above property of the CC formalism (referred to as the CC downfolding) is valid for *any type of subalgebra*  $\mathfrak{h}$  [henceforth referred to as the subsystem embedding subalgebras (SES)] described above. The partitioning of the cluster operator into internal and external parts has been originally introduced in the context of the state-selective multireference CC formalism in Refs. [34–37]. Although the SES theorem [Eq. (5)] and equivalence theorem (see below) are based on the decomposition of cluster operator into internal or external parts, the possibility of calculating CC energies in an alternative way and integrating various active-space problems were proposed only recently [23,32]. The invariance of the CC energy with respect to the choice of SES led to the concept of quantum flow and equivalence theorem [23,38], which states that when several SES problems represented by (6) are coupled into the flow, i.e.,

$$H^{\text{eff}}(\mathfrak{h}_i)e^{T_{\text{int}}(\mathfrak{h}_i)}|\Phi\rangle = Ee^{T_{\text{int}}(\mathfrak{h}_i)}|\Phi\rangle (i = 1, \dots, M) \quad (7)$$

( $M$  stands for the number of CASs included in the flow), the corresponding solution is equivalent to the standard representation of the CC theory given by Eqs. (3) and (4) with the  $T$  operator defined as a combination of all nonrepetitive excitations included in  $T_{\text{int}}(\mathfrak{h}_i)$  ( $i = 1, \dots, M$ ) operators, symbolically denoted as

$$T = \sum_{i=1}^M T_{\text{int}}(\mathfrak{h}_i). \quad (8)$$

An important consequence of the equivalence theorem is the fact that for some choices of cluster operator, Eq. (8), high-dimensionality problem, Eqs. (3) and (4) can be replaced by a flow composed of reduced dimensionality

non-Hermitian eigenvalue problems. For each subalgebra  $\mathfrak{h}_i$  in the eigenvalue problem of Eq. (7), the effective Hamiltonian  $H^{\text{eff}}(\mathfrak{h}_i)$  follows Eq. (6), where the external cluster operators  $T_{\text{ext}}(\mathfrak{h}_i)$  are the collection of operators excluding  $T_{\text{int}}(\mathfrak{h}_i)$ ,

$$T_{\text{ext}}(\mathfrak{h}_i) = T - T_{\text{int}}(\mathfrak{h}_i). \quad (9)$$

The  $T$  operator defined by Eq. (8) does not correspond, in general, to a typical rank-truncated cluster operator. For example, for all possible (4e,4o)-type active spaces, the  $T$  operator encompasses all single and double excitations as well as subsets of triple and quadruple. A version of the equivalence theorem holds for truncated forms of  $T_{\text{int}}(\mathfrak{h}_i)$  operators, which leads to the recovery of standard rank-defined CC approximations. However, in this case, the active-space problems cannot be represented in an elegant form involving effective Hamiltonian language.

To extend the SR-CC flows to the Hermitian case, in contrast to previous analysis [23], we will employ variational principle using functional

$$E = \langle\Phi|e^{-\sigma}He^{\sigma}|\Phi\rangle, \quad (10)$$

where a general-type anti-Hermitian cluster operator  $\sigma$  ( $\sigma = \sum_{k=1}^{N_A} [1/(k!)]^2 \sum_{q_1, \dots, q_k}^{p_1, \dots, p_k} \sigma_{p_1, \dots, p_k}^{q_1, \dots, q_k} a_{q_1}^\dagger \dots a_{q_k}^\dagger a_{p_k} \dots a_{p_1}$ ,  $\sigma^\dagger = -\sigma$ ) includes all excitations needed to generate space that is too large to be handled by available quantum computers. To tackle the problem using limited quantum resources, let us assume that the  $\sigma$  operator can be approximated by amplitudes included in anti-Hermitian operators  $\sigma_{\text{int}}(\mathfrak{h}_i)$  ( $i = 1, \dots, M$ ), producing excitations within corresponding active spaces [ $AS(i)$ ] generated by subalgebras  $\mathfrak{h}_i$

$$\sigma \simeq \sum_{i=1}^M \sigma_{\text{int}}(\mathfrak{h}_i). \quad (11)$$

In the next step, we will look at the problem (10) from the point of view of  $i$ th active space and decompose  $\sigma$  operator as

$$\sigma \simeq \sigma_{\text{int}}(\mathfrak{h}_i) + \sigma_{\text{ext}}(\mathfrak{h}_i), \quad (12)$$

and

$$E = \langle\Phi|e^{-\sigma_{\text{int}}(\mathfrak{h}_i) - \sigma_{\text{ext}}(\mathfrak{h}_i)}He^{\sigma_{\text{int}}(\mathfrak{h}_i) + \sigma_{\text{ext}}(\mathfrak{h}_i)}|\Phi\rangle. \quad (13)$$

Next, we will utilize the order- $N$  active-space-specific Trotter formula (in analogy to Ref. [23]) to expand exponents, which introduce active-space-specific  $E(\mathfrak{h}_i)$  approximation to energy  $E$ :

$$E(\mathfrak{h}_i) = \langle\Psi_{\text{int}}(\mathfrak{h}_i, N)|H^{\text{eff}}(\mathfrak{h}_i, N)|\Psi_{\text{int}}(\mathfrak{h}_i, N)\rangle, \quad (14)$$

where

$$H^{\text{eff}}(\mathfrak{h}_i, N) = [P + Q_{\text{int}}(\mathfrak{h}_i)][G_i^{(N)}]^{-1} H G_i^{(N)} [P + Q_{\text{int}}(\mathfrak{h}_i)] \quad (15)$$

$$G_i^{(N)} = (e^{\sigma_{\text{ext}}(\mathfrak{h}_i)/N} e^{\sigma_{\text{int}}(\mathfrak{h}_i)/N})^{N-1} e^{\sigma_{\text{ext}}(\mathfrak{h}_i)/N} \quad (16)$$

and

$$|\Psi_{\text{int}}(\mathfrak{h}_i, N)\rangle = e^{\sigma_{\text{int}}(\mathfrak{h}_i)/N} |\Phi\rangle. \quad (17)$$

The coupled variational problems (14) for  $i = 1, \dots, M$  define the QFlow algorithm. As in the non-Hermitian case, the total pool of amplitudes optimized in the QFlow corresponds to all nonrepetitive amplitudes for active spaces included in the flow. As a consequence of the noncommutativity of operators defining  $\sigma$  operators and the need to use Trotter approximations, the energy values in (14) may be, in general different. For this purpose, we introduce physically motivated ordering of the active spaces [the first (last), or primary active space contains the most (the least) important part of correlation effects] based, for example, on the orbital energy criteria and use the energy  $[E(\mathfrak{h}_i)]$  to probe the energy in the QFlow procedure. The advantage of the quantum version of the QFlow algorithm stems from the fact that the qubits requirement is associated with the qubits requirement of the largest active space in the flow. In this Letter, we will mainly focus our attention on the simplest  $N = 1$  case where sets of amplitudes defining effective Hamiltonian and  $|\Psi_{\text{int}}(\mathfrak{h}_i, N = 1)\rangle \equiv |\Psi_{\text{int}}(\mathfrak{h}_i)\rangle$  are disjoint.

*Numerical implementation.*—The QFlow algorithm has never been validated numerically. To fill this gap, we developed QFlow implementation for the first-order Trotterization approximation ( $N = 1$ ) based on the stringMB code—an occupation number representation-based emulator of quantum computing [33]. Our QFlow implementation, which emulates a VQE solver for each CAS involved in the flow, is schematically shown in Fig. 1 and uses conventional computers to store a global pool of amplitudes and prepare effective Hamiltonian for each cycle. When representing the flow in the form of coupled eigenvalue problems, one has the flexibility in defining the active spaces, which can include those that overlap with each other and share common parameters. For the  $\mathfrak{h}_i$  computational block we partition the set of variational parameters  $\theta(\mathfrak{h}_i)$  into subset  $\theta^{\text{CP}}(\mathfrak{h}_i)$  that refers to common pool of amplitudes determined in preceding steps [say, for  $\mathfrak{h}_j (j = 1, \dots, i - 1)$ ] and subset  $\theta^{\text{X}}(\mathfrak{h}_i)$  that is uniquely determined in the  $\mathfrak{h}_i$  minimization step for  $E(\mathfrak{h}_i)$ , i.e.,

$$\min_{\theta^{\text{X}}(\mathfrak{h}_i)} \langle \Psi_{\text{int}}(\theta^{\text{X}}(\mathfrak{h}_i), \theta^{\text{CP}}(\mathfrak{h}_i)) | H^{\text{eff}}(\mathfrak{h}_i) | \Psi_{\text{int}}(\theta^{\text{X}}(\mathfrak{h}_i), \theta^{\text{CP}}(\mathfrak{h}_i)) \rangle, \quad (i = 1, \dots, M), \quad (18)$$

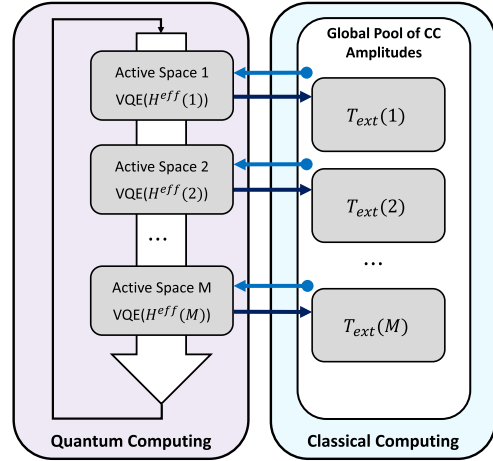


FIG. 1. Schematic representation of the QFlow algorithms. All cluster amplitudes [global pool of CC amplitudes; (GPA)] are residing on classical computers. The effective Hamiltonians are formed on classical computers using GPA and encoded on quantum computers (light blue arrows). Quantum computers use these Hamiltonians to optimize internal excitations for a given active space and are used to update GPAs (dark blue lines).

where  $H^{\text{eff}}(\mathfrak{h}_i) \equiv H^{\text{eff}}(\mathfrak{h}_i, N = 1)$  and  $|\Psi_{\text{int}}(\theta^{\text{X}}(\mathfrak{h}_i), \theta^{\text{CP}}(\mathfrak{h}_i))\rangle$  (chosen in the form of unitary CC (UCC) Ansatz [39–41]) approximates  $|\Psi_{\text{int}}(\mathfrak{h}_i)\rangle = e^{\sigma_{\text{int}}(\mathfrak{h}_i)} |\Phi\rangle$  in Eq. (17). When combined with a simple form of the gradients estimates on the quantum computers [14]

$$\frac{\partial E(\mathfrak{h}_i)}{\partial \theta^{\text{X}}(\mathfrak{h}_i)_k} \simeq \langle \Psi_{\text{int}}(\mathfrak{h}_i) | [H^{\text{eff}}(\mathfrak{h}_i), \tau_k^{\text{X}}(i)] | \Psi_{\text{int}}(\mathfrak{h}_i) \rangle, \quad (19)$$

where  $\tau_k^{\text{X}}(i)$  is a corresponding combination of the strings of a creation/annihilation operators associated with the  $\theta^{\text{X}}(\mathfrak{h}_i)_k$  amplitude in the  $\sigma_{\text{int}}(\mathfrak{h}_i)$  operator. Instead of performing full optimization for each active space included in the QFlow, we perform only one optimization step based on the gradient (19). We also employ UCC-type representation for each  $\sigma_{\text{ext}}(\mathfrak{h}_i)$  needed to construct  $H^{\text{eff}}(\mathfrak{h}_i)$  operator in Eq. (15).

*Results.*—As test systems to demonstrate the performance of the QFlow techniques, we chose the  $H_n$  linear chains of the hydrogen atoms: H6 and H8 models in small STO-3G basis set [42], where one can vary the complexity of the ground-state wave function by changing the H-H distances ( $R_{\text{H-H}}$ ) between adjacent atoms. For example, while for  $R_{\text{H-H}} = 2.0$  a.u., one deals with the weakly correlated case, for  $R_{\text{H-H}} = 3.0$  a.u., the system is strongly correlated and all Hartree-Fock orbitals used in simulations are non-negligible. This means that one cannot define a single small-dimensionality active space to capture all needed correlation effects for the  $R_{\text{H-H}} = 3.0$  a.u. case. Recently, the  $H_n$  models have been used for validation of cutting-edge many-body numerical methodologies for treating correlated quantum systems [43–47].

TABLE I. Converged QFlow energies (in Hartree) for H6 and H8 benchmark systems at  $R_{\text{H-H}} = 2.0$  and  $R_{\text{H-H}} = 3.0$  a.u. corresponding to weakly and strongly correlated regimes, respectively.

Method	H6 (2.0 a.u.)	H6 (3.0 a.u.)	H8 (2.0 a.u.)	H8 (3.0 a.u.)
HF	-3.1059	-2.6754	-4.1382	-3.5723
CAS-ED	-3.1669	-2.8021	-4.1906	-3.6656
CCSD	-3.2173	-2.9673	-4.2848	-3.9727
CCSDT	-3.2180	-2.9692	-4.2867	-3.9784
CCSDTQ	-3.2177	-2.9574	-4.2860	-3.9439
QFlow(4e,4o) <sup>a</sup>	-3.2173	-2.9521	-4.2847	-3.9322
ED	-3.2177	-2.9576	-4.2860	-3.9447

<sup>a</sup>QFlow energies are reported from the primary active space consisting of the two highest energy occupied orbitals and two lowest energy unoccupied orbitals.

We summarized QFlow results in Table I and in Figs. 2 and 3. For both systems, the QFlow included all active spaces defined by arbitrary two occupied active and two virtual active orbitals and four active electrons [the QFlow (4e,4o) model]. For H6 and H8 systems QFlow integrates 9 and 36 active spaces, respectively. In Table I, the QFlow (4e,4o) results are compared against exact diagonalization (ED) in the full space, in the primary active space (CAS-ED) consisting of the two highest energy occupied orbitals and two lowest energy unoccupied orbitals, and typical CC approximations including excitations from singles to quadruples (CCSD, CCSDT, and CCSDTQ) [31]. It is evident that the QFlow algorithm significantly reduces errors of the CAS-ED method—a prevailing model for performing quantum simulations on NISQ-type devices. In the extreme case, the error of CAS-ED amounting to 279 mHartree for the H8 3.0 a.u. system is reduced by QFlow to 12.4 mHartree. Additionally, it should be noticed that for the H6 and H8  $R_{\text{H-H}} = 3.0$  a.u. models, the CCSD and CCSDT formulations experience variational collapse placing the ground-state energies significantly below the ED ones. For weakly correlated H6 and H8 models ( $R_{\text{H-H}} = 2.0$  a.u.), the QFlow results are within chemical accuracy error bars (less than 1.59 mHartree). In Fig. 2, we show energies [ $E(\mathfrak{h}_i)$ ] calculated in the first four QFlow cycles for two geometries of H8. In both cases, we can observe that energies obtained in the first non-trivial cycle (second cycle) are considerably better than the CAS-ED energy for the primary active spaces (targeted in typical VQE simulations).

In Fig. 3, we discuss the discrepancies between the minimum and maximum values of  $E(\mathfrak{h}_i)$  for each cycle for H8 3.0 a.u. model. Despite the fact that in cycles two and three these discrepancies are substantial, in the following iterations, these discrepancies significantly decrease. For 20th cycle, the discrepancy is less than 2.0 mHartree, which indicates that despite approximations associated with the

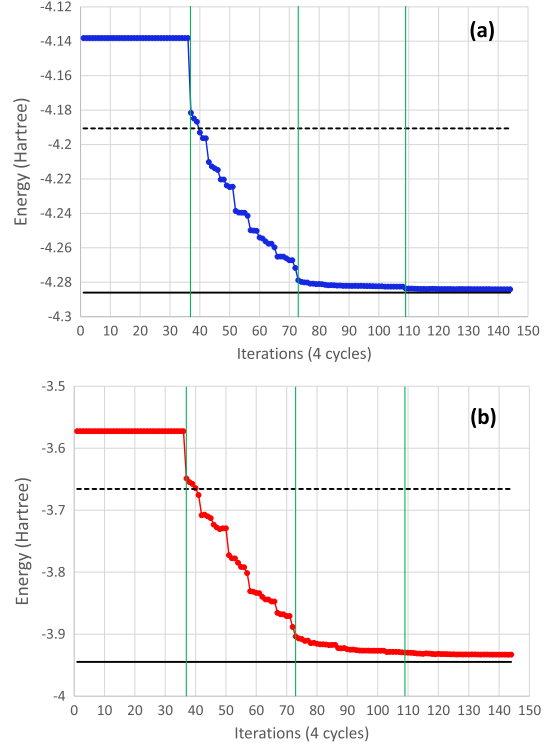


FIG. 2. Energy evaluations (for all active spaces) in the QFlow for STO-3G H8 model: (a)  $R_{\text{H-H}} = 2.0$ , blue circles, (b)  $R_{\text{H-H}} = 3.0$  a.u., red circles. The dotted and solid horizontal black lines correspond to the active-space and full-space exact diagonalizations, respectively. We report the energies of all active space problems for the first four cycles, where the start of each cycle is indicated by the green vertical lines. To initiate the optimization process, we utilized a zero vector as the initial guess for all active spaces. The optimization process is based on the gradients (19), and the update of the parameter pool starts from the second cycle. Thus, all energies in the first cycle correspond to HF energies.

non-commutative characters of cluster operators in QFlow, the energy invariance of the SR-CC flow (7) at the solution is approximately satisfied. This discrepancy is further

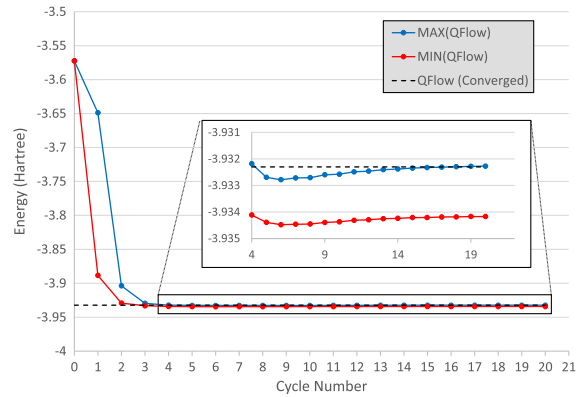


FIG. 3. The minimum and maximum values of  $E(\mathfrak{h}_i)$  at the beginning of each QFlow cycle of the STO-3G H8  $R_{\text{H-H}} = 3.0$  a.u. model.



TABLE II. The DUCC-QFlow energies (in Hartree) for the H6 model ( $R_{\text{H-H}} = 3$  a.u.) in the cc-pVDZ basis set.

Method	Energy
CCSD	-3.1571
CCSDT	-3.1619
CCSDTQ	-3.1591
DUCC(6act)-QFlow(4e,4o)	-3.1570
DUCC(7act)-QFlow(4e,4o)	-3.1589
ED	-3.1591

reduced to the 0.2 mHartree by order-3 ( $N = 3$ ) Trotter expansion for the effective Hamiltonians (15) [at the same time order-3 expansion reduces order-1 QFlow(4e,4o) error of 12.5 mHartree for H8 3 a.u. model to 9.7 mHartree]. In the QFlow simulations for the H8 system, we optimized 684 parameters using coupled computational blocks corresponding to active space eigenvalue problems that optimize at most 35 parameters. Concurrently, the number of QFlow optimized amplitudes is considerably lower than that of CCSDTQ ones. For instance, QFlow optimizes only 36 quadruply excited amplitudes, while the CCSDTQ approach utilizes 1810 of them (with no spatial symmetry invoked in both techniques).

While the STO-3G basis set is useful for validating the QFlow algorithm, in practical applications, larger basis sets that properly capture short-range dynamical correlation effects are required. To address this challenge, we have implemented a two-step strategy, referred to as the DUCC-QFlow approach described in Ref. [23]. This approach utilizes (i) classical computers and a simplified downfolding technique to evaluate an approximate form of the effective Hamiltonian ( $A$ ) for active spaces that are too large for current quantum hardware, and (ii) quantum computers to solve the problem described by Eq. (10) with  $H$  replaced by  $A$  using the QFlow algorithm. We illustrate the feasibility of the DUCC-QFlow algorithm in handling larger basis sets on the challenging example of H6 for  $R_{\text{H-H}} = 3$  a.u. for cc-pVDZ basis set [48] and active orbitals defined by six [DUCC(6act)-QFlow(4e,4o)] and seven [DUCC(7act)-QFlow(4e,4o)] lowest Hartree-Fock orbitals. As a downfolding procedure for the first step, we adopted the A(7) approximation for the downfolding technique of Ref. [49]. The DUCC-QFlow results shown in Table II indicate that while DUCC(6act)-QFlow(4e,4o) provides accuracies of the CCSD energies, the DUCC(7act)-QFlow(4e,4o) furnishes energies in a good agreement with the CCSDTQ or ED results.

*Summary.*—We provided numerical evidence that the QFlow algorithm can efficiently sample large subspaces of the Hilbert space through coupled variational problems in reduced dimensionality active spaces. Using very modest active space sizes, we illustrated the utility of the QFlow procedure with the STO-3G H6 and H8 hydrogen chains in weakly and strongly correlated regimes with errors within

chemical accuracy for weakly correlated systems and relatively small errors for the strongly correlated systems. For the strongly correlated H8 model, we recover nearly 97% of the correlation using active spaces containing small number of optimized parameters compared to the exact diagonalization. Additionally, the application of the two-step DUCC-QFlow protocol successfully accounted for correlation effects in the highly correlated version of the H6 molecule utilizing a larger cc-pVDZ basis set. Our expectations are that the DUCC-QFlow algorithm will facilitate the seamless integration of classical and quantum computational resources.

The examples in this Letter are very conservative estimates of the dimensionality reduction that can be achieved with the QFlow algorithm. As quantum technology evolves and we transition from the noisy intermediate-scale quantum devices era to fully fledged error-corrected quantum computing, the ability to adapt to new methodological advances and efficiently utilize hybrid computational resources is ever important. An intriguing aspect of QFlow, to be explored in forthcoming studies is the possibility to (i) employ the local character of correlation effects, and (ii) construct adaptive QFlow approaches involving a preselected set of various-size active spaces relevant to the problem of interest [50–54]. This has the potential to overcome the limitations of models based on all possible fixed-size active spaces for large-scale applications. Moreover, preliminary tests suggest that modifying the QFlow by optimizing all active space problems simultaneously, rather than using a serial-type algorithm, produces equivalent optimized energy and comparable convergence patterns, enabling the development of efficient parallel or distributed QFlow algorithms. The authors expect that the QFlow algorithm demonstrated in this Letter will play an important role in pushing the envelope of many-body applications as quantum computing continues to evolve.

This material is based upon work supported by the “Embedding QC into Many-body Frameworks for Strongly Correlated Molecular and Materials Systems” project, which is funded by the U.S. Department of Energy, Office of Science, Office of Basic Energy Sciences, the Division of Chemical Sciences, Geosciences, and Biosciences (under FWP 72689) and by Quantum Science Center (QSC), a National Quantum Information Science Research Center of the U.S. Department of Energy (under FWP 76213). This work used resources from the Pacific Northwest National Laboratory (PNNL). PNNL is operated by Battelle for the U.S. Department of Energy under Contract No. DE-AC05-76RL01830.

\*karol.kowalski@pnnl.gov

[1] M. A. Nielsen and I. L. Chuang, *Quantum Computation and Quantum Information: 10th Anniversary Edition*, 10th ed. (Cambridge University Press, New York, NY, USA, 2011).

- [2] A. Y. Kitaev, [arXiv:quant-ph/9511026](#).
- [3] A. Y. Kitaev, *Russ. Math. Surv.* **52**, 1191 (1997).
- [4] D. S. Abrams and S. Lloyd, *Phys. Rev. Lett.* **83**, 5162 (1999).
- [5] A. M. Childs, *Commun. Math. Phys.* **294**, 581 (2010).
- [6] M. Reiher, N. Wiebe, K. M. Svore, D. Wecker, and M. Troyer, *Proc. Natl. Acad. Sci. U.S.A.* **114**, 7555 (2017).
- [7] A. Peruzzo, J. R. McClean, P. Shadbolt, M.-H. Yung, X.-Q. Zhou, P. J. Love, A. Aspuru-Guzik, and J. L. O'Brien, *Nat. Commun.* **5**, 4213 (2014).
- [8] J. R. McClean, J. Romero, R. Babbush, and A. Aspuru-Guzik, *New J. Phys.* **18**, 023023 (2016).
- [9] J. Romero, R. Babbush, J. R. McClean, C. Hempel, P. J. Love, and A. Aspuru-Guzik, *Quantum Sci. Technol.* **4**, 014008 (2018).
- [10] A. Kandala, A. Mezzacapo, K. Temme, M. Takita, M. Brink, J. M. Chow, and J. M. Gambetta, *Nature (London)* **549**, 242 (2017).
- [11] A. Kandala, K. Temme, A. D. Córcoles, A. Mezzacapo, J. M. Chow, and J. M. Gambetta, *Nature (London)* **567**, 491 (2019).
- [12] A. F. Izmaylov, T.-C. Yen, R. A. Lang, and V. Verteletskyi, *J. Chem. Theory Comput.* **16**, 190 (2019).
- [13] R. A. Lang, I. G. Ryabinkin, and A. F. Izmaylov, *J. Chem. Theory Comput.* **17**, 66 (2021).
- [14] H. R. Grimsley, S. E. Economou, E. Barnes, and N. J. Mayhall, *Nat. Commun.* **10**, 3007 (2019).
- [15] H. R. Grimsley, D. Claudino, S. E. Economou, E. Barnes, and N. J. Mayhall, *J. Chem. Theory Comput.* **16**, 1 (2019).
- [16] S. McArdle, S. Endo, A. Aspuru-Guzik, S. C. Benjamin, and X. Yuan, *Rev. Mod. Phys.* **92**, 015003 (2020).
- [17] W. M. Kirby and P. J. Love, *Phys. Rev. Lett.* **127**, 110503 (2021).
- [18] J. Tilly, H. Chen, S. Cao, D. Picozzi, K. Setia, Y. Li, E. Grant, L. Wossnig, I. Rungger, G. H. Booth *et al.*, *Phys. Rep.* **986**, 1 (2022).
- [19] T. Takeshita, N. C. Rubin, Z. Jiang, E. Lee, R. Babbush, and J. R. McClean, *Phys. Rev. X* **10**, 011004 (2020).
- [20] B. Şahinoğlu and R. D. Somma, *npj Quantum Inf.* **7**, 119 (2021).
- [21] J. Liu, Z. Li, and J. Yang, *J. Chem. Theory Comput.* **18**, 4795 (2022).
- [22] N. P. Bauman, E. J. Bylaska, S. Krishnamoorthy, G. H. Low, N. Wiebe, C. E. Granade, M. Roetteler, M. Troyer, and K. Kowalski, *J. Chem. Phys.* **151**, 014107 (2019).
- [23] K. Kowalski, *Phys. Rev. A* **104**, 032804 (2021).
- [24] F. Coester, *Nucl. Phys.* **7**, 421 (1958).
- [25] F. Coester and H. Kummel, *Nucl. Phys.* **17**, 477 (1960).
- [26] J. Čížek, *J. Chem. Phys.* **45**, 4256 (1966).
- [27] J. Paldus, J. Čížek, and I. Shavitt, *Phys. Rev. A* **5**, 50 (1972).
- [28] J. Arponen, *Ann. Phys. (N.Y.)* **151**, 311 (1983).
- [29] R. F. Bishop and H. Kummel, *Phys. Today* **40**, No. 3, 52 (1987).
- [30] J. Paldus and X. Li, *Adv. Chem. Phys.* **110**, 1 (1999).
- [31] R. J. Bartlett and M. Musiał, *Rev. Mod. Phys.* **79**, 291 (2007).
- [32] K. Kowalski, *J. Chem. Phys.* **148**, 094104 (2018).
- [33] K. Kowalski, *J. Chem. Phys.* **158**, 054101 (2023).
- [34] P. Piecuch, N. Oliphant, and L. Adamowicz, *J. Chem. Phys.* **99**, 1875 (1993).
- [35] P. Piecuch and L. Adamowicz, *J. Chem. Phys.* **100**, 5792 (1994).
- [36] L. Adamowicz, P. Piecuch, and K. B. Ghose, *Mol. Phys.* **94**, 225 (1998).
- [37] P. Piecuch, *Mol. Phys.* **108**, 2987 (2010).
- [38] N. P. Bauman and K. Kowalski, *Mater. Theory* **6**, 1 (2022).
- [39] R. J. Bartlett, S. A. Kucharski, and J. Noga, *Chem. Phys. Lett.* **155**, 133 (1989).
- [40] A. G. Taube and R. J. Bartlett, *Int. J. Quantum Chem.* **106**, 3393 (2006).
- [41] F. A. Evangelista, *J. Chem. Phys.* **134**, 224102 (2011).
- [42] W. J. Hehre, R. F. Stewart, and J. A. Pople, *J. Chem. Phys.* **51**, 2657 (1969).
- [43] L. Li, T. E. Baker, S. R. White, and K. Burke, *Phys. Rev. B* **94**, 245129 (2016).
- [44] M. Motta, D. M. Ceperley, G. K.-L. Chan, J. A. Gomez, E. Gull, S. Guo, C. A. Jiménez-Hoyos, T. N. Lan, J. Li, F. Ma *et al.*, *Phys. Rev. X* **7**, 031059 (2017).
- [45] D. Pfau, J. S. Spencer, A. G. D. G. Matthews, and W. M. C. Foulkes, *Phys. Rev. Res.* **2**, 033429 (2020).
- [46] N. H. Stair and F. A. Evangelista, *J. Chem. Theory Comput.* **153**, 104108 (2020).
- [47] I. Magoulas, J. Shen, and P. Piecuch, *Mol. Phys.* **120**, e2057365 (2022).
- [48] T. H. Dunning Jr, *J. Chem. Phys.* **90**, 1007 (1989).
- [49] N. P. Bauman and K. Kowalski, *J. Chem. Phys.* **156**, 094106 (2022).
- [50] J. Olsen, B. O. Roos, P. Jørgensen, and H. J. A. Jensen, *J. Chem. Phys.* **89**, 2185 (1988).
- [51] T. Fleig, J. Olsen, and C. M. Marian, *J. Chem. Phys.* **114**, 4775 (2001).
- [52] J. Ivanic, *J. Chem. Phys.* **119**, 9364 (2003).
- [53] T. Sato and K. L. Ishikawa, *Phys. Rev. A* **91**, 023417 (2015).
- [54] D. Ma, G. Li Manni, and L. Gagliardi, *J. Chem. Phys.* **135**, 044128 (2011).